Habitable Planet, 2026, 2(1), 14–28

Habitable Planet

Journal Homepage: https://www.sciltp.com/journals/hp

Article

Metallogeny vis-à-vis Proterozoic Tectonics of the Central Indian Tectonic Zone (CITZ): An Overview

M. Lachhana Dora [1,2,*], Ranjit Rath [3,4] and Kirtikumar Randive [5]

[1] School of Environmental Sciences, Jawaharlal Nehru University, New Delhi 110067, India
[2] Geological Survey of India, Nagpur 440006, India
[3] Oil India Limited (OIL), NCR, Noida 201301, India
[4] Geological Survey of India, Kolkata 700016, India
[5] PG Department of Geology, RTM Nagpur University, Nagpur 440033, India
* Correspondence: dorageol@gmail.com

ABSTRACT

This work presents a synthesis of mineral deposits formed during the evolution of the Central Indian Tectonic Zone (CITZ). The CITZ is situated between the Bundelkhand and Bastar cratons, representing a major Proterozoic orogenic suture that preserves a complex record of tectonic, magmatic, metamorphic, and metallogenic (M3) events during the ~2.4–0.9 Ga period. The CITZ encompasses a diverse tectonic belt, represented by the Mahakoshal in the north, the Betul in the central sector, and the Sausar belt in the south. The tectonic evolution of the CITZ records a protracted history of intraplate magmatism, rifting, oceanic crust generation, arc-back-arc development, and continental-margin accretion, and culminated with the final collision of the two Archean cratons of Peninsular India. This convergence-driven evolution (2.1–1.6 Ga) is reflected in distinct mineralization events that define the metallogeny of the CITZ. The earliest metallogenic phase is marked by Fe-graphite-orogenic gold mineralization in the Mahakoshal belt and graphite in the Betul belt, linked to the initial collision of the Bundelkhand and Bastar cratons (1.95–1.80 Ga). Subsequently, volcanogenic massive sulfide (Zn–Pb ± Cu) deposits were formed during 1.80–1.70 Ga in the Betul belt, associated with multiple stages of arc-rifting. The Sausar belt evolved into a world-class manganese metallogenic province, reflecting basin-scale sedimentary and diagenetic processes operating during the Paleoproterozoic and Neoproterozoic. The waning stages of intraoceanic arc development were accompanied by emplacement of voluminous mafic–ultramafic flows and sills, hosting Ni–Cu–PGE prospects at Padhar complex in the Betul belt. Later, the phase is associated with alkali magmatism, which led to REE mineralization.

ARTICLE INFO

History:

Received: 30 September 2025
Revised: 10 October 2025
Accepted: 19 October 2025
Published: 24 October 2025

Keywords:

Central Indian Tectonic Zone (CITZ);
Metallogeny;
Proterozoic geodynamics;
Supercontinents

Citation:

Dora, M.L.; Rath, R.; Randive, K. Metallogeny vis-à-vis Proterozoic Tectonics of the Central Indian Tectonic Zone (CITZ): An Overview. Habitable Planet **2026**, 2(1), 14–28. https://doi.org/10.63335/j.hp.2025.0023

Research Highlights

- Central Indian Tectonic Zone (CITZ) is a suture between Bundelkhand-Bastar craton
- Mahakoshal, Betul, and Sausar belts within CITZ show world-class mineral systems
- Mineral systems formed by collision, arc, rift, and alkaline magmatism processes
- Integrated study in CITZ shows graphite, Au, VMS, Mn, Ni-PGE, and REE potential
- ~1.4 Ga metallogenic history of CITZ is linked to Columbia-Rodinia supercontinent

1. Introduction

The Proterozoic Era (2.4–0.5 Ga) marks a distinctive period in Earth's evolution, characterized by fundamental changes in continental plate configurations, tectonic processes [1,2], and shifts in ocean and atmospheric composition [3,4]. Within this global tectonic framework, the Central Indian Tectonic Zone (2.4–0.9 Ga) represents a trans-continental suture along which the major crustal blocks of peninsular India, Northern Block (Bundelkhand and Aravalli cratons) and the Southern Block (Dharwar, Bastar, and Singhbhum cratons) amalgamated (Figure 1a) [5–7].

The CITZ encompasses three major Proterozoic supracrustal belts: (1) the Mahakoshal belt in the north, (2) the Betul belt in the central part, and (3) the Sausar belt in the south (Figure 1b). These tectonic zones experienced multiple episodes of subduction, collision, and accretionary orogenesis during the Proterozoic [6,8,9]. Its prolonged polyphase history of magmatism, sedimentation, metallogeny, and orogenesis, spanning from the Paleoproterozoic (~1.8 Ga) to the Neoproterozoic, is well documented in the literature, but its evolution is still under debate [5,10–12]. Systematic geological mapping at 1:50,000 and 1:25,000 scales by the Geological Survey of India during the late 1980s and 1990s, followed by regional mineral exploration during 2020–2023, facilitated follow-up exploration and detailed metallogenic studies across the CITZ. From a metallogenic perspective, the CITZ hosts a range of mineral systems formed in different tectonic and magmatic settings [13–16]. Four to five broad mineral systems can be distinguished based on geodynamic setting: (i) world-class manganese deposits of the Sausar Belt (e.g., Balaghat, Tirodi, Mansar, Dongribuzuru), (ii) volcanogenic massive sulfide (VMS) deposits of the Betul Belt (e.g., Mouriya, Bhuyari, etc.) [17–19] (iii) Fe-graphite mineralization in the Betul and Mahakoshal belt [20,21] (iv) orogenic lode-gold deposits (Gurhar Pahar, Chakariya) of the Mahakoshal belt [15,16] (v).Critical minerals like Ni-PGE-REE in Betul (Padhar) [22] and REE in the Sausar belt [23] (Deolapar area).

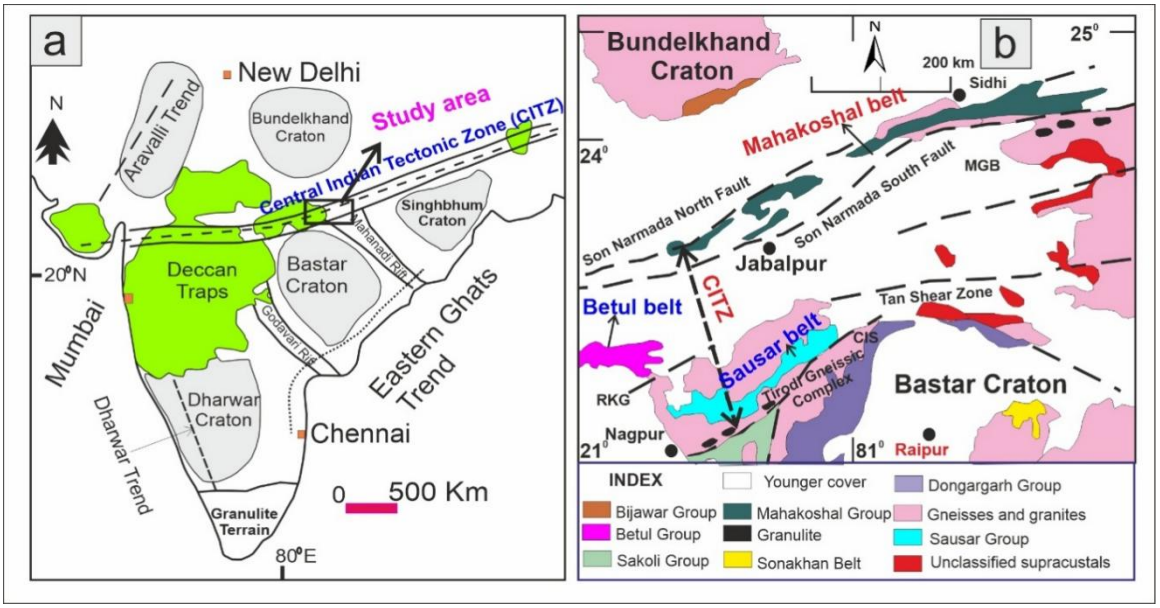

Figure 1. (**a**) Geotectonic evolution of India with inset box showing the location of the CITZ, modified after [24] (**b**). The regional geological map demonstrating the structural framework and major Proterozoic supracrustal belts, namely Mahakoshal, Betul, and Sausar, within the Central Indian Tectonic Zone (CITZ), modified after [25–27].

A substantial amount of research has been carried out on tectonics, granite magmatism, and metamorphism within the CITZ, and numerous studies have been published on these aspects [5–7]. However, relatively little attention has been paid to its metallogeny. Our study presents an overview of the Precambrian metallogeny of the CITZ, with a focus on mineralization in relation to the region's evolving tectonic, stratigraphic, metamorphic, and magmatic frameworks. The Central Indian Tectonic Zone (CITZ), with its remarkable geological diversity, traversed with numerous shear zones and complex polyphase metallogenic evolution, holds significant potential for critical metal resources such as graphite, REE, Cd, Bi, and Co. A comprehensive understanding of the CITZ's metallogenic framework provides a crucial foundation for integrating resource development with the principles of sustainability and a circular economy. An advanced exploration of these metals is vital to strengthening India's self-reliance in strategic sectors.

Following a brief geological overview, the mineralization associated with Paleoproterozoic to

Neoproterozoic units is examined to address key aspects of ore genesis, when, where, and why mineral deposits formed through their spatial, temporal, and lithochemical characteristics within the broader CITZ outline. We did an integrated summary of metallogeny in the context of tectono-magmatic and metamorphic events that shaped the Central Indian Orogen during the Proterozoic (2.2–0.8 Ga). Here, metallogeny is considered in terms of the spatial and temporal distribution of mineral deposits, their relationships to geological units, and their genesis within the CITZ framework. All information was sourced from academic papers and technological project reports. As an overview, this research paper does not cover every detail of the tectonic and metallogenic evolution of the three belts. However, the references cited will guide readers to more detailed sources. The scope of this communication is also limited to the geological framework of well-known mineral deposits and prospects within CITZ (Table 1), while comprehensive inventories of all known mineral prospects and occurrences can be found in detailed compilations by the Geological Survey of India, miscellaneous publications of Maharashtra and Madhya Pradesh [26,27], memoirs, and dossiers available on the GSI portal (www.gsi.gov.in).

Table 1. Summarised distribution and characteristics of major mineral resources across the tectonic units of the Central Indian Tectonic Zone (CITZ), compiled from key prospects and deposits.

Mineral Belts within CITZ	Important Mineral Deposits and Prospects Name	Host Rocks Characteristics.	Nature of Mineralization	Alterations Types	Ore Mineral Assemblages	Tentative Ages (Ga)
Mahakoshal Belt (MB)	Gurhar Pahar, Chakariya Imaliya, Bagda	BIF, phyllite, dolomite of Agori Parsoi Formations	Shear zone hosted Au associated with sulfides in quartz–carbonate veins.	Chloritisation, Seritisation, Dolomitisation,	Asp, Po, Ccp, Py, Au, Bi	Paleoproterzoic (1.9–1.7 Ga)
Betul Belt (BB)	Bhuyari, Mouriya, Koparpani, Bhawaratekra, Tarora, Biskhan, Jangaldehri,	Rhyolites, metabasalts	VMS-types, massive and vein type Zn–Cu–Pb hosted in foliated rhyolites.	Chloritisation, Seritisation, Dolomitisation, Fe-Mg-Ca alteration, Fe-Al alteration.	Sp, Cu, Gn, Py, Po	Paleoproterzoic (1.8–1.7 Ga)
Sausar Belt (SB)	Kandri, Dongriburuzug, Tirodi, Balaghat, Ukwa	Mica-schist and carbonates	Syn-sedimentary type, Stratiform Mn		Braunite-bixbyite-hausmannite–hollandite-jacobsite assemblages; supergene enrichment forming pyrolusite, psilomelane	1.9–1.8 (?) 1.0–0.9 (?)

2. Geologic Setting of the CITZ

2.1. Regional Tectonic Framework

The Central Indian Tectonic Zone (CITZ) extends E–W to ENE–WSW for >800 km, with a maximum width of ~400 km [9,28]. The lithotectonic assemblage comprises a supracrustal belt, granulite terranes, mafic–ultramafic bodies, TTG gneisses, charnockites, arc-related suites, metacarbonates, BIFs and Mn formations, a high-pressure and ultrahigh-temperature metamorphic belt, and post-collisional K-rich granites [6,29].

Several crustal-scale parallel shear zones define the CITZ: the Central Indian Shear (CIS), Gavilgarh–Tan Shear Zone, Son–Narmada South Fault (SNSF), and Son–Narmada North Fault (SNNF) (Figure 1b). The Mahakoshal belt lies between the SNNF and SNSF, while the Gavilgarh–Tan Shear Zone separates the Sausar and Betul belt; the CIS forms the southern limit (Figure 1b).

The tectonic evolution of the CITZ remains debated. Early models invoked southward subduction of the northern block beneath the southern block along the CIS [30,31], while ref. [25] argued for north-directed subduction of the southern block beneath the northern block at ~1500 Ma, forming the Ramakona–Katangi granulite belt as an accretionary orogen. High-grade metamorphic records from the Balaghat–Bhandara granulites and Tirodi biotite gneiss suggest multiple accretionary cycles with slab rollback [32]. More recently, refs. [5–7] proposed a prolonged orogenic evolution between 2.5 and 0.85 Ga, involving both the Bundelkhand and Bastar cratons.

2.2. Geological Outlines of the Three Belts

2.2.1. Mahakoshal Belt

The Mahakoshal belt extends from Hoshangabad, Madhya Pradesh, in the west to Palamau, Jharkhand, in the east. The Mahakoshal belt is made up of metavolcanic and metasedimentary rocks belonging to the Sleemanabad (=Agori), Parsoi, and Dudhamaniya formations in ascending order [26,33–35] (Figure 2).

The supracrustal sequence is dominated by metasediments with subordinate metavolcanics mainly of tholeiitic composition. The belt is also exposed to granitoids, mafic–ultramafic intrusions, BIFs, carbonatites, syenites, and lamprophyres [36,37]. This supracrustal belt has been considered a rift setting [38] and a. 2.1 Ga back-arc setting [39]. Volcanics of dacitic-rhyolitic composition (~1.89 Ga) and associated alkaline intrusions are also documented [12,40,41]. Granitoids such as the Madanmahal granite (1.6–1.7 Ga [42] and the Barambara–Jhirgadandi granites (1.75 Ga; U–Pb SHRIMP zircon; [43] intruded into metasediments. Structurally, the belt records multiple deformation events and two distinct metamorphic phases M1–D1 (~1.9–1.8 Ga) and M2–D2 (~1.8–1.7 Ga) [11]. These processes play a key role in gold and graphite mineralization. Field observations, petrographic analyses, and subsequent electron microprobe studies confirm the occurrence of gold associated with arsenopyrite and scorodite (Figures 2c,d and 3a–c).

2.2.2. Betul Belt

The Betul belt (BB) is a Precambrian gneiss–supracrustal inlier and extends ~135 km ENE–WSW between Chicholi (west) and Chhindwara (east) (GSI, 2014) [26]. The BB is tectonically bounded by the Sausar belt (south) and the Mahakoshal belt (north) [16,21,44,45] (Figure 4).

The BB remains largely unexplored in terms of geochronological constraints. Recently, ref. [6] combined field observations with isotopic (Sr–Nd, U–Pb zircon, CHIME monazite) and geochemical data to reconstruct the geological evolution of the Betul belt (2.2–0.85 Ga) and establish its links with Proterozoic supercontinent cycles. This includes biotite gneisses (~2.1 Ga), pillow basalts (~2.0 Ga), rhyolites (~1.7 Ga), exhalites, quartzites, metapelites, and calc-silicates, intruded by granites (~1.6 Ga) [6]; syenites, and mafic–ultramafic bodies [22,46,47].Volcano-sedimentary rocks in the eastern and central belt host VMS-type base metal mineralization (Figure 4) [17,48,49] and references therein) and metasediments with BIF and graphite mineralization in the western part of the Betul belt [20] (Figure 4). The rocks record three phases of deformation and regional metamorphism from granulite to amphibolite facies, overprinted locally by greenschist facies [26,27,50,51].

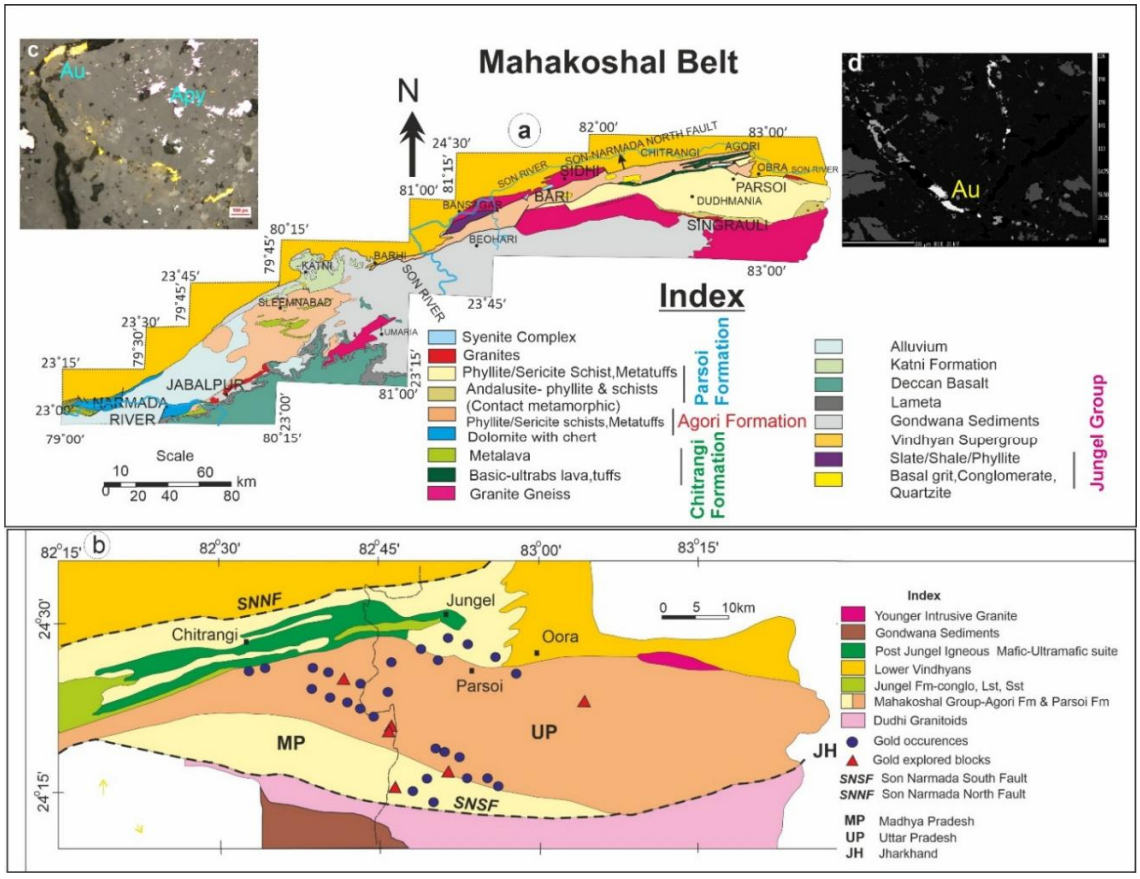

Figure 2. (**a**) Regional geological map of the Mahakoshal Belt showing major lithotectonic units and gold prospects modified after [26]. (**b**) Distribution of gold prospects and exploration blocks [35]. (**c**,**d**) Petrographic and electron probe microanalysis (EPMA) BSE images showing the occurrence of gold grains along micro-fractures within the host quartz mineral.

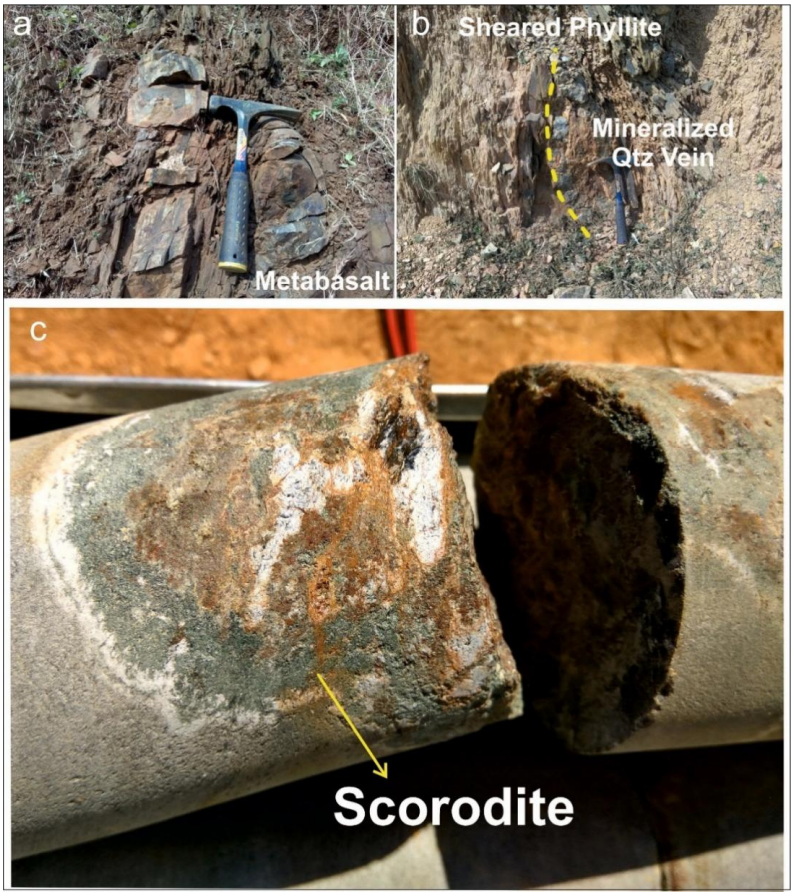

Figure 3. (**a**,**b**) Field exposures showing sheared metabasalt and mineralized quartz veins localized along the S_1 and S_2 foliation planes within phyllites; (**c**) Drill core sample illustrating the alteration of arsenopyrite into porous, light bluish-green scorodite within phyllitic host rock.

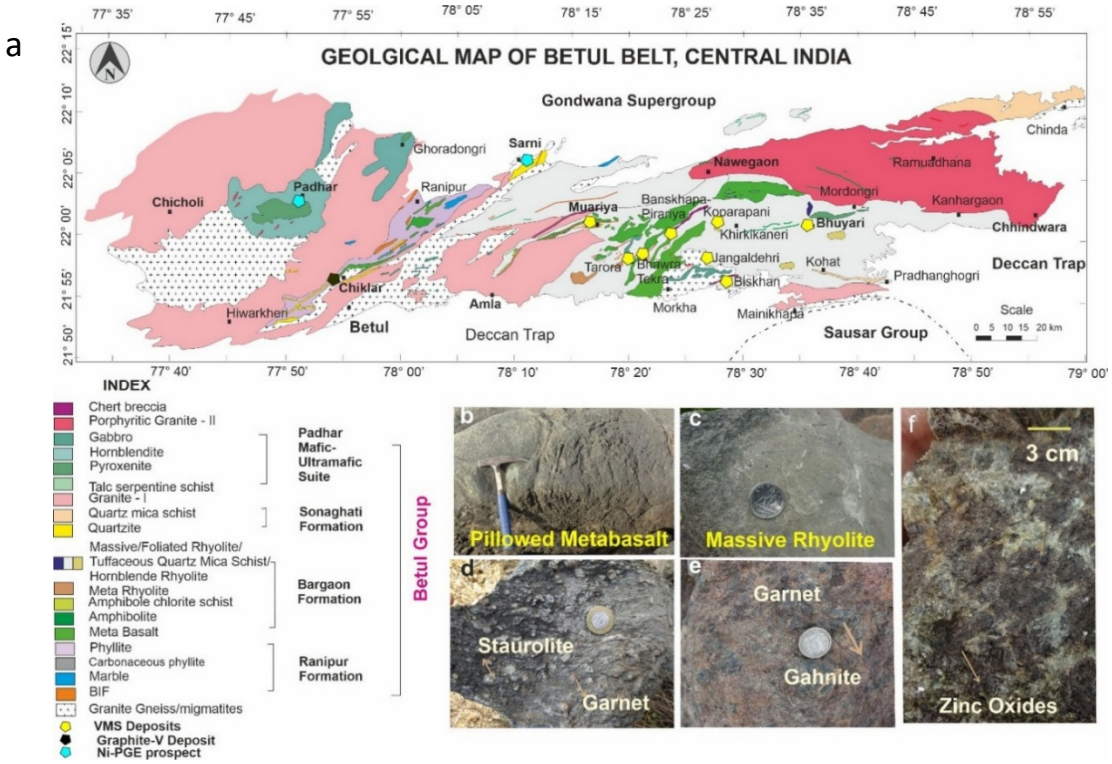

Figure 4. (**a**) Regional geological map of the Betul Belt illustrating the distribution of pillow lavas, felsic volcanics within basement gneisses, VMS deposits, and associated mafic-felsic intrusions (modified after Dora et al., 2023 [6]). (**b**–**f**) Field photographs depicting key lithological variants and their spatial relationship with VMS-type mineralization in the Betul Belt, Central Indian Tectonic Zone (CITZ).

2.2.3. Sausar Belt

The Sausar Group forms an arcuate belt (~215 km long, ~35 km wide) extending from Kachidhana (Chhindwara District, MP) to Ukwa (Balaghat District, MP), passing through Nagpur and Bhandara (Maharashtra) (Figure 5) [27]. The general strike varies from WNW–ESE (west) to E–W (central) and NE–SW (east). The belt includes two major units: the Tirodi biotite gneiss (TG) and the Sausar Group (SG) [23,52–54]. The TBG is an Archean felsic gneiss complex with enclaves of metabasic and granulite-facies rocks, overlain unconformably by the Sausar Group, marked by a paleosol horizon of 2.5–2.2 Ga and basal conglomerate [55]. The Sausar Group of Palaeoproterozoic age comprises a thick sequence of carbonate-quartzite-psammopelitic rocks rich in manganese-bearing rocks called gondites formed during 2.2 to 1.8 Ga. The belt has undergone significant polyphase deformation, resulting in complex fold patterns and a general ENE-WSW alignment, associated with Mn mineralization. Subsequent deformation, metamorphism, and remobilisation took place during Meso–Neoproterzoic the Meso-Neoproterozoic period (1.5–1.4 Ga, 1.0–0.9 Ga, and 0.6–0.5 Ga) [55,56].

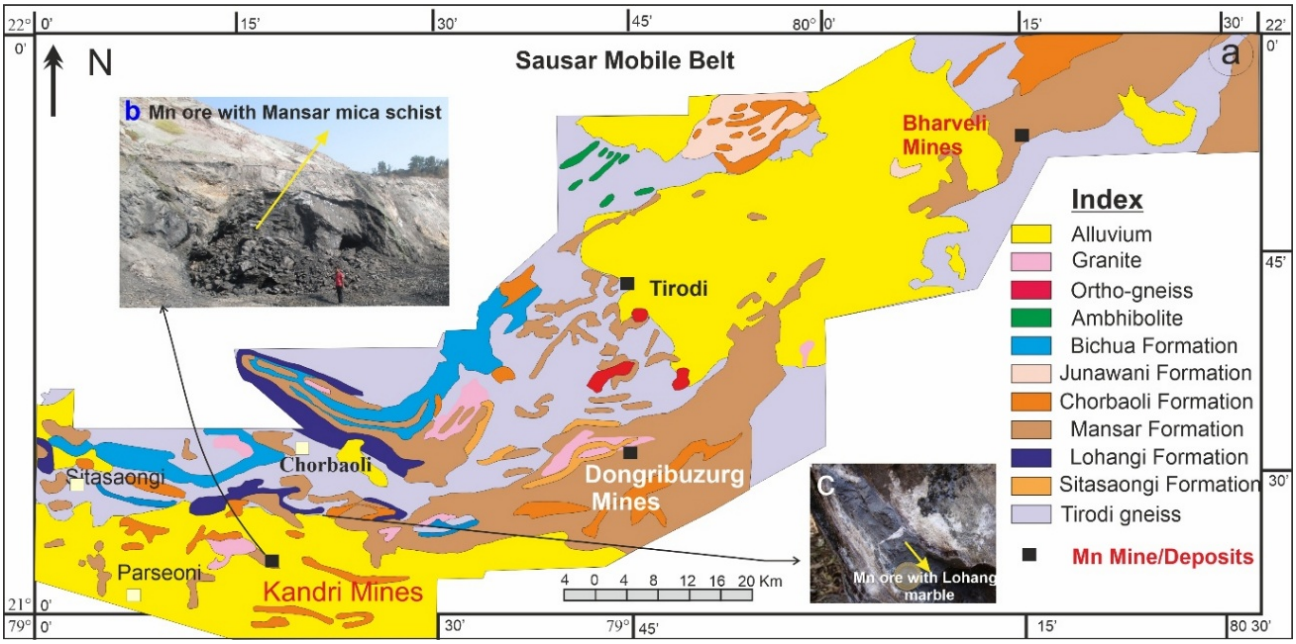

Figure 5. (**a**) Regional geological map of the Sausar Belt showing the distribution of metasedimentary sequences and basement gneisses modified after [26,27,52,54]. (**b**,**c**) Field photographs illustrating Mn mineralization hosted within the Mansar mica schist and Lohangi marble units of the Sausar Belt, Central Indian Tectonic Zone (CITZ).

3. Regional Metallogeny

3.1. Metallogeny in the Mahakoshal Belt (MB)

Gold and graphite mineralization typically occur in quartz–carbonate veins localized along shear and dilational zones within folded and sheared volcanics, volcaniclastic, and metasedimentary sequences of the Agori and Parsoi formations (Figure 2) [15,35,57]. Gold mineralization occurs in three geological conditions: (1) syngenetic type with BIF in the eastern part, i.e., Sonkuswa; (2) epigenetic type with phyllites in the central part (Gurhar Pahar, Bagada), and (3) dolomite-hosted in the western part (Imaliya) [16,35,57,58]. Surface indications of mineralization are rare, but specks, blebs, thin bands, and stringers of arsenopyrite and scorodite occur in oxidized quartz veins along fractures in the Chakariya, Gurhar Pahar, Bagada, and Nawanagar areas (Figures 2 and 3). Scorodite forms light yellow-green grains that weather to limonite, marking secondary dispersion haloes (Figure 3d). GSI [26] has established resources at Gurhar Pahar (7.29 Mt @ 1.03 g/t Au), Chakariya (0.137 Mt @ 1.81 g/t Au), and Imaliya (0.35 Mt @ 1.13 g/t Au) [35].

3.2. Metallogeny in Betul Belt (BB)

Sulfide mineralization and syn-volcanic hydrothermal alteration in the Betul belt are linked to submarine bimodal volcanism [17,19,49,59]. Felsic volcaniclastics serve as the main host rocks in most deposits. Alteration zones have been metamorphosed to middle to upper-amphibolite facies, resulting in diverse metamorphic mineral assemblages, such as phlogopite-biotite-chlorite-garnet-gahnite-sericite (Figure 4). The BB exhibits approximately 2051 ± 80 Ma (Sm–Nd) age for pillowed basalt and about 1715±10 Ma (U-Pb zircon) for rhyolite [6]. A Pb model age of roughly 1800

Ma has been reported from galena in VMS mineralization at Bhuyari [19]. Extensive exploration between 1990 and 2005 identified rhyolite-hosted Zn–Cu–Pb mineralization at Mouriya, Ghisi (west), Dehalwara, Banskhapa-Pipariya, Koparpani, Bhawaratekra, Tarora (central), and Biskhan, Jangaldehri, Borkhap, Bhuyari (east) [18,19,60–62].

The base metal mineralization is exposed in the eastern and central parts of this belt, whereas graphite deposits are mainly concentrated in the suprarustals of the western part of the Betul inlier, specifically in Chiklar-Gauthana-Tikari, Golighat-Junewani, and Bhopali areas [20]. Mafic–ultramafic magmatism occurs at Padhar, Ghoradongri, and Mordongri, producing pyroxenite, gabbro, and diorite intrusives, which are associated with Ni-PGE mineralization [6,22,47,63,64]. The BB was intruded by two distinct phases of granite (1.6 Ga and 0.9 Ga), the younger one is associated with REE mineralization [6].

3.3. Metallogeny in Sausar Belt (SB)

The SB hosts India's largest and richest Mn ore deposits within low- to high-grade metamorphosed Sausar Group metasediments [52,53,65]. Major deposits include Mansar, Tirodi, Dongri Buzurg, Bharweli, and Chikla, distributed over >200 km strike length. Manganese occurs conformably within the Mansar (pelitic) and Lohangi (calcareous) formations, co-folded with gondite rocks (Figure 5). Mn ores occur as oxides, carbonate–oxide lenses, and silicate admixtures. Mineralogically, they comprise braunite, bixbyite, hausmannite, hollandite, jacobsite, vredenburgite, pyrolusite, cryptomelane, and psilomelane [65]. Supergene enrichment produced pyrolusite, rhodonite, and cryptomelane–psilomelane assemblages [56]. The Sausar sediments were deposited in a stable shelf setting, with Mn carbonates diagenetically derived from oxides under evaporitic conditions, while silicate admixtures reflect detrital influx [53,65]. REE mineralization has been documented in the late-stage granites and associated pegmatites [23].

4. Discussion

4.1. Crustal Evolution of the CITZ

The CITZ records a protracted polyphase evolution marked by multiple cycles of volcanism, sedimentation, deformation, metamorphism, and magmatism throughout the Proterozoic [5–7,66–68]. The earliest, approximately 2.16 Ga granitoid gneisses display arc-related geochemical signatures, suggesting Paleoproterozoic subduction-related magmatism that occurred alongside early collision between the Bundelkhand and Bastar cratons [6,33,42]. Older inherited zircons (2.73–2.53 Ga) indicate involvement of Archean Bundelkhand crust [69]. Seismic and magnetotelluric studies support the northward subduction of Bastar beneath Bundelkhand [70]. Subduction- related mafic volcanism (2.08–1.84 Ga) and related sediments of the Betul and Mahakoshal belt formed in arc–back- arc settings [39,47,64]. A later rifting phase (~1.80–1.67 Ga) is recorded by rhyolite and A-type granites, such as the Morkha granite, in the Betul belt [6]. Closure of the Betul basin around 1.6–1.5 Ga was marked by continent–continent collision, along with ultramafic–mafic magmatism in the Padhar–Mordongri area [47]. Regional metamorphism at approximately 1.32–1.40 Ga developed in the CITZ [68]. This phase also involved granulite exhumation driven by crustal thickening and rapid decompression. The overlying Sausar supracrustals were deposited on the combined cratonic basement. The Neoproterozoic period is characterized by the emplacement of Navegaon granite (1.07–0.95 Ga) [6]. and Sausar granites, which occurred concurrently with peak metamorphism of Sausar sediments [66–68]. This event correlates with the approximately 1.1.0–0.9 Ga Sausar Orogeny, although it is not well documented in the Mahakoshal belt [25]. The CITZ reflects the result of complex tectonic processes involving crustal thinning, rifting, and passive margin development, followed by accretion, convergence, and continent–continent collision, broadly correlating with the Columbia and Rhodinia supercontinent cycles (Figure 6).

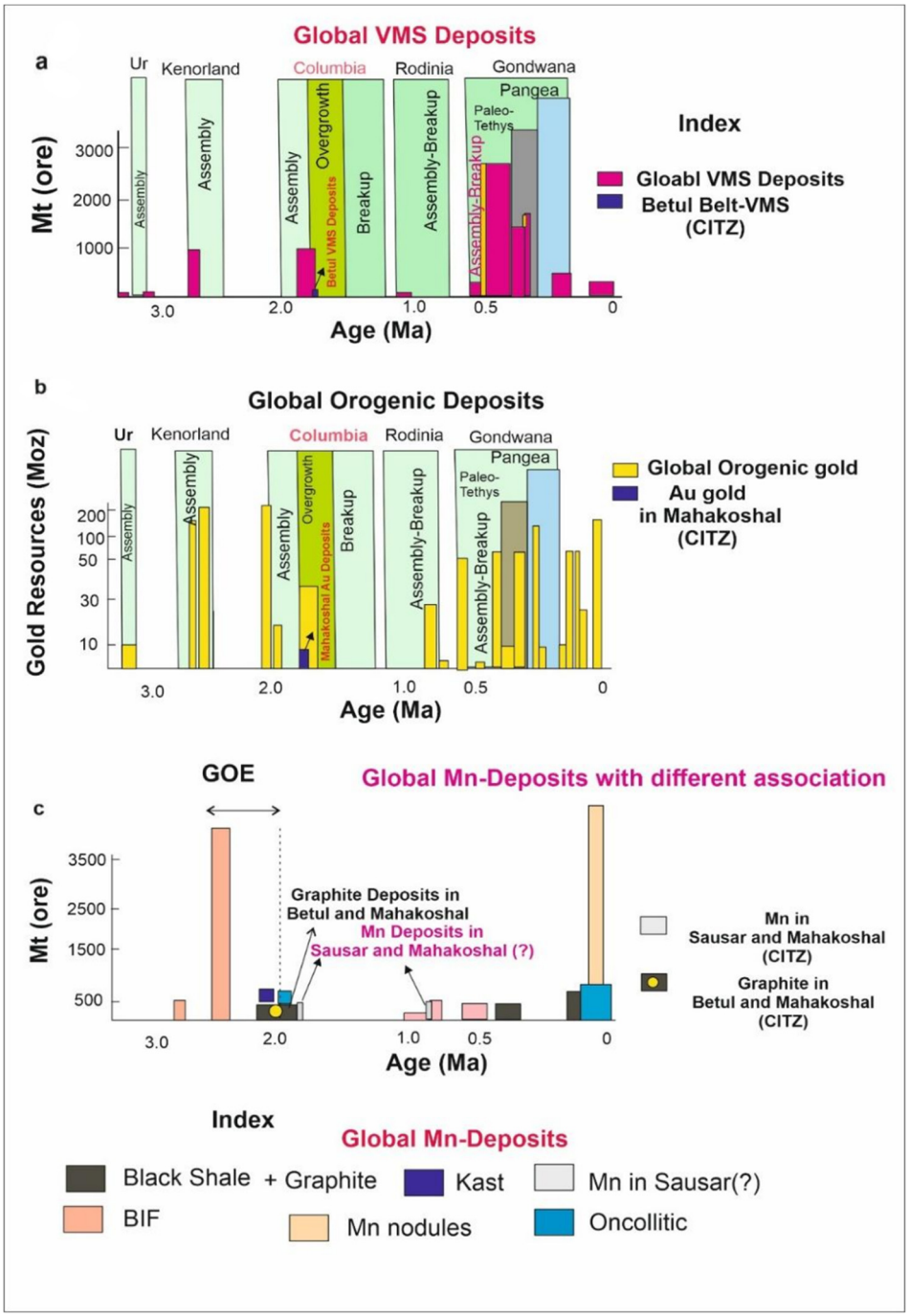

Figure 6. Temporal distribution of major mineral systems formed through Earth's history in subduction-related convergent margin settings, illustrated within the framework of the supercontinent cycle modified after [71]. (**a**) VMS Cu–Zn–Pb systems modified after [72]; (**b**) Orogenic gold systems modified after [73] and (**c**) Manganese mineral systems linked to the Great Oxidation Event (GOE), modified after [72].

4.2. Metallogeny within the CITZ

The CITZ records a long tectonic history from Paleoproterozoic subduction–collision to Neoproterozoic extension, marked by multiple orogenic, magmatic, and metamorphic events that generated diverse mineralization styles (Au, graphite, Fe, Mn, VMS, Ni–PGE, REE, Figure 6). These episodes fostered favorable mineral systems and drove regional hydrothermal fluid circulation along brittle to brittle–ductile shear zones in all three belts. Though timing is poorly constrained for mineralization events, available geochronology indicates that craton convergence and subsequent felsic-mafic magmatism were the main fluid drivers, leading to varied mineral systems. A few key deposits and their likely origins within the CITZ are discussed below:

4.2.1. Metallogenesis of Orogenic Gold in the Mahakoshal Belt

Gold mineralization in the Mahakoshal belt occurs mainly in sheared quartz–carbonate veins with

sulfides, hosted in metavolcanic–metasedimentary rocks of the Agori and Parsoi formations [14,26,35,57]. Sulfides include pyrite, pyrrhotite, arsenopyrite, sphalerite, and minor bismuth. Mineralization is linked to ~1.89 Ga Parsoi metavolcanics [41] granitic activity, deformation, and metamorphism between 1.9–1.7 Ga [11], suggesting Fe–graphite–gold deposition at 1.9–1.8 Ga. This coincides with the Bundelkhand–Bastar craton collision, providing crustal-scale fluid pathways and structural traps within the CITZ during the Columbia assembly. Regional studies [15,16,35,57] confirm structurally controlled orogenic-type mineralization. Globally, gold peaks show at 2.75–2.55 Ga (Kenorland; [71–73] and 2.16–2.03 Ga (Birimian) [74] (Figure 6). The 1.9–1.8 Ga Mahakoshal event represents Columbia-related localized orogenic gold mineralization (Figure 6).

4.2.2. Genesis of BIF and Mn in the Mahakoshal and Betul Belt

Iron formations of the Mahakoshal supracrustal belt occur in a volcano-sedimentary rift basin (Nair et al., 1995 [33]), with deposits located at Kochita, Jhoko, Bhainsahiya, Kosomhar, Charki, Umreha, and Nimoura [75]. Their interlayering with ~1.89 Ga metavolcanics and phyllites suggests a syn-volcanic setting, later modified by hydrothermal activity. Comparable BIF/hematite–magnetite quartzites occur in the Ranipur Formation, Betul belt. Globally, major BIF deposition peaked at 2.6–2.4 Ga during Kenorland and the Great Oxidation Event (GOE; ~2.4 Ga). Mahakoshal BIFs (~1.9–1.8 Ga) formed during waning GOE stages, producing small, restricted basin deposits [71] (Figure 6).

4.2.3. Metallogenesis of Graphite-V in the Betul and Mahakoshal Belt

Graphite mineralization (>8% FC) with vanadium occurs in the western Betul belt along the Sonaghati shear zone (Chiklar–Gauthana–Tikari, Golighat–Junewani, Bhopali), linked to carbonaceous sediment deposition in shelf–basin settings [20]. Shale, chert, and limestone preserved organic matter, later recrystallized to graphite during ca. 2.1–2.0 Ga collisional orogeny under progressive P–T conditions. Globally, major graphite mineralization formed during Archean–Paleoproterozoic high-grade metamorphism, with smaller events in later orogenies. Within CITZ, graphite also occurs in ca. 1.9 Ga carbonaceous phyllites of the Agori Formation, Mahakoshal belt [21], reflecting syngenetic sedimentary precursors modified epigenetically during orogenesis (Figure 6).

4.2.4. Metallogenesis of VMS deposits in the Betul Belt

Volcanic-hosted massive sulfide (VMS) mineralization in the Betul belt formed at ~1.8 Ga within submarine volcano-sedimentary basins in a back-arc rift setting [6,19]. Bimodal felsic volcanics, cherts, and carbonaceous rocks record synvolcanic hydrothermal circulation, where seawater-derived fluids leached Zn–Cu–Pb–Fe and deposited stratiform to stratabound sphalerite–chalcopyrite–galena lenses at Bhuyari, Mourya, Bhawaratekra, etc. Subsequent deformation and metamorphism modified ore textures [17]. Detailed studies include refs. [17–19,44,45,49]. Globally, such VMS systems characterize submarine hydrothermal activity in extensional settings [71,76] with Betul representing a Paleoproterozoic similarity within CITZ metallogeny (Figure 6).

4.2.5. Genesis of Mn deposits in the Sausar and Mahakoshal Belt

Manganese deposits of the Sausar belt formed in a Paleoproterozoic basin, where Mn-rich chemical sediments of the Mansar–Lohangi Formation accumulated under oxygen-deficient to mildly oxidizing conditions. The Satpura orogeny metamorphosed these to amphibolite–granulite facies, producing high-grade assemblages (spessartine, manganocummingtonite, braunite, hausmannite, bixbyite). Structural deformation upgraded ores into lenticular, folded, and shear-controlled bodies across M.P. and Maharashtra [53,65]. Mn prospects also occur with Fe in the Agori Formation, Mahakoshal belt. Globally, Mn deposition shifted from pre-GOE carbonates to post-GOE shales/oolitic types [71,77]. Sausar Mn deposits fit the Paleoproterozoic Mn metallogenic window, coeval with Mahakoshal (~1.9 Ga) within CITZ.

4.2.6. Metallogenesis of Critical Metals (Ni-PGE-REE)

Critical metals include Ni–PGE–REE mineralization that occurs in mafic–ultramafic intrusions and associated tectono-magmatic events within CITZ. In the Mahakoshal belt, lamproite and carbonatite from the Chitrangi region, Jungel valley provide favorable settings for Ni-REE mineralization, related to Paleoproterozoic rift-controlled magmatism [78]. The Betul belt records multiphase mafic–ultramafic and granite intrusions emplaced within a Proterozoic volcano-sedimentary sequence, where disseminated sulfide mineralization carries Ni–Cu with significant PGE and REE associations, suggesting mantle-derived arc magmatism linked to Columbian supercontinent cycles [22,47] (Figures 4 and 5). In the Sausar Belt, extensive granitic and alkaline magmatism, along with associated hydrothermal activity, is well documented. Rare Earth Element (REE) mineralization occurs in late phase granite and pegmatites formed during the final collision between

the Bastar and Bundelkhand cratons in the time of the Rodinia supercontinent [23] (Figure 5).

4.3. Tectonic Controls on Metallogeny in the CITZ and their Global Significance

The CITZ preserves a multiphase record of tectono-magmatic and metamorphic events recognized through field, petrographic, geochemical, isotopic, and geochronological studies, many synchronous with global orogenic cycles [5–7]. U–Pb zircon ages from Betul granite gneiss (central part of CITZ) indicate intracrustal melting at ca. 2.16 Ga, with inherited 2.72 Ga components suggesting felsic protoliths comparable to Bundelkhand gneisses [6,47]. This supports prolonged amalgamation of Bundelkhand and Bastar cratons via northward subduction [12,25,42] (Figure 7). Subsequent arc-related volcanism at ca. 2.0 Ga in the Betul and Mahakoshal belt reflects Paleoproterozoic accretionary processes linked to Columbia assembly [39,79,80]. Iron formations in the Betul-Mahakoshal belt (1.90–1.80 Ga) and gold metallogeny in Mahakoshal coincide with the Columbia assembly and multi-source fluid-induced hydrothermal systems, matching a few deposits in the Trans-Hudson orogen, Baltic Shield, and North Australia [73]. Late Paleoproterozoic magmatism (1.8–1.65 Ga), including rhyolites and anorogenic granites in the Betul belt associated with VMS deposits, reflects the Columbia breakup and matches the Capricorn Orogeny in Western Australia [81,82]. Mafic intrusions in the Padhar complex (1.32–1.24 Ga; [6] with minor Ni–PGE highlight crustal extension during Columbia breakup [22,47,67]. Late-stage alkaline granites (1.07–0.95 Ga) reported from Betul and Sausar correspond to the Rodinia assembly [6,9,66–68,83]. The ca. 1.07 Ga Grenvillian imprint in Betul and Sausar parallels Canada, Eastern Ghats, and Rayner Complex [84], marking the final India–Antarctica–Australia suturing [6,11,55]. These orogens share similar tectonic characteristics, including thrusting, crustal-scale shear zones, and syn-collisional magmatism associated with REE metallogeny noticed in the Sausar and Betul belt [23,85,86]. Thus, the CITZ preserves a 2.16–0.95 Ga history of accretion, collision, rifting, plume activity, and late orogenesis, controlling the distribution of Fe, Mn, base, and precious metal deposits, more comparable to the Bryah–Padbury basins of the Capricorn Orogen (Figure 7) [81].

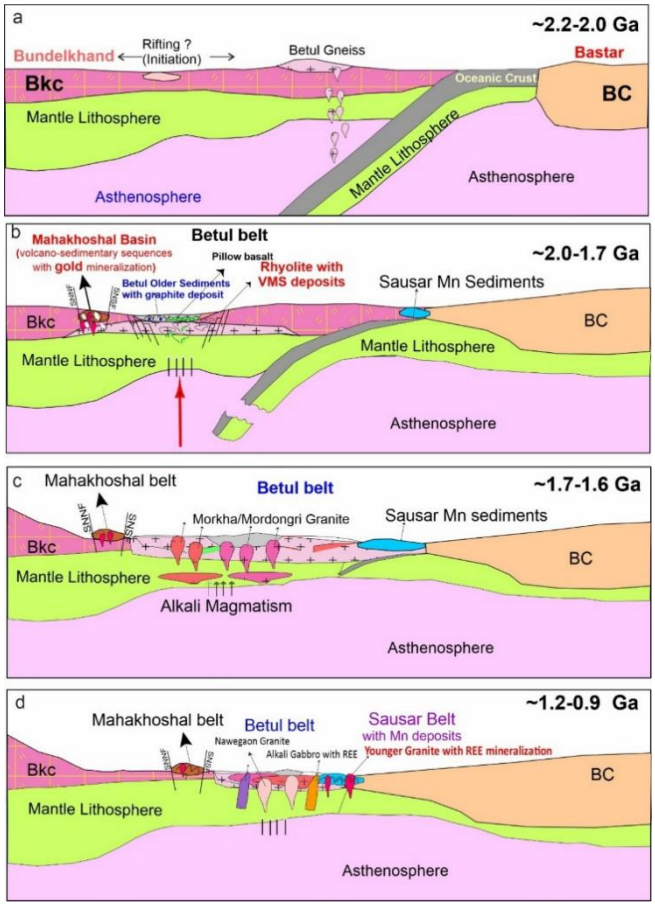

Figure 7. (**a**–**d**) Sketch geological model (not to scale) depicting the complex tectono-magmatic evolution of the Central Indian Tectonic Zone (CITZ), modified after [6].

4. Summary and Conclusions

The Central Indian Tectonic Zone (CITZ) marks a major Proterozoic suture between the Bundelkhand and Bastar cratons, forming a metallogenically rich belt whose geological evolution is closely tied to global cycles of supercontinent assembly, breakup, and crustal reworking. Integrated studies covering field geology, petrography, mineral and bulk rock geochemistry, fluid inclusion analysis, stable isotope systematics, and geochronology from key lithounits lead to several important conclusions about regional metallogeny. The Central Indian Tectonic Zone records the earliest suturing between the North Indian Craton (NIC) and South Indian Craton (SIC) around 2.10 to 2.00 Ga (Figure 7), following an initial accretionary phase (>2.16 Ga) and subsequent subduction-related arc magmatism between 2.00 and 1.80 Ga. Mineral systems linked with sedimentary and volcanic processes within the zone are associated with ocean-floor magmatism, basin development, and hydrothermal exhalation. Structurally controlled lode systems formed under compressional conditions, including orogenic gold and polymetallic sulfide deposits in the Mahakoshal Belt, graphite deposits in

Betul, BIF-hosted iron in Mahakoshal, and manganese deposits in the Sausar Belt. Later extensional tectonics between 1.80 and 1.60 Ga triggered rhyolitic volcanism and the emplacement of A-type granites, leading to VMS-style sulfide mineralization. Shallow marine sedimentation in the Sausar basin promoted manganese accumulation, which was later enriched by Meso- to Neoproterozoic metamorphism and hydrothermal alteration. Post-collisional extension (~0.95–0.93 Ga) was characterized by alkaline magmatism and associated REE mineralization. These tectono-magmatic events align with the assembly and breakup of the Columbia and Rodinia supercontinents and the Grenvillian orogeny, highlighting the Central Indian Tectonic Zone's importance as a key node in the global Precambrian crustal evolution and metallogeny.

In summary, the zone represents a major polyphase metallogenic belt offering vital insights into the relationship between orogenic activity, supercontinent cycles, and mineralization patterns in central India, underscoring the need for ongoing exploration, research, and resource assessment.

Author Contributions

M.L.D.: Conceptualization, Investigation, Methodology, Writing-original draft. R.R.: Review and editing. K.R.: Review and editing. All authors have read and agreed to the published version of the manuscript.

Funding

This research received no external funding.

Institutional Review Board Statement

Not applicable.

Informed Consent Statement

Not applicable.

Data Availability Statement

All data used in this study are presented in the paper.

Conflicts of Interest

The authors declare no conflict of interest, and they have no known competing financial interests or personal relationships that could have appeared to influence the work reported in this paper.

Acknowledgments

We extend sincere gratitude and thank M. Santosh, Executive Advisor, Habitable Planet Journal, for kindly inviting us to contribute to the theme on Metallogeny in CITZ. It is a privilege to be associated with the inaugural volumes of such a promising journal.

Due acknowledgment has been given to the Geological Survey of India for providing all facilities to conduct this research work at CITZ over the last two decades under various field season programs. MLD expresses sincere gratitude to Shri Asit Saha, Tushar Meshram, Shri S. R. Baswani, and Gladsen Bage (GSI) for their invaluable support during the fieldwork in the Mahakoshal belt. Two anonymous reviewers are thanked for their insightful comments to improve the manuscript.

Use of AI and AI-Assisted Technologies

The authors have used Chat GPT and Grammarly for language improvement.

References

1. Rogers, J.J.W.; Santosh, M. Tectonics and surface effects of the supercontinent Columbia. *Gondwana Res.* **2009**, *15*, 373–380. https://doi.org/10.1016/j.gr.2008.06.008
2. Wang, Z.; Zhang, J.; Zong, K.; et al. Plate tectonics: The stabilizer of Earth's habitability. *J. Earth Sci.* **2023**, *34*, 1645–1662. https://doi.org/10.1007/s12583-023-1864-9
3. Anbar, A.D.; Knoll, A.H. Proterozoic ocean chemistry and evolution: A bioinorganic bridge? *Science* **2002**, *297*, 1137–1142. https://doi.org/10.1126/science.1069651
4. Santosh, M. Habitable Planet Earth: Secular evolution and sustainable future. *Habitable Planet* **2025**, *1*, 286–297. https://doi.org/10.63335/j.hp.2025.0021
5. Sharma, A.; Chakraborty, P.P.; Pandey, A.K.; et al. A tale of evolution of the Central Indian Tectonic Zone (CITZ) with glimpses on pre-suture plate margin depositional history. *Geol. J.* **2025**, *60*, 404–430. https://doi.org/10.1002/gj.5087
6. Dora, M.L.; Meshram, T.; Baswani, S.R.; et al. Geological evolution of the Proterozoic Betul belt (~2.16–0.95 Ga) of the Central Indian Tectonic Zone: Its linkage to the assembly and dispersal of Columbia and Rodinia supercontinents. *Gondwana Res.* **2023**, *116*, 168–197. https://doi.org/10.1016/j.gr.2022.11.017
7. Mohanty, S.P.; Li, Q.; Zhai, M.; et al. Geochronology of post-tectonic granite and gneiss of the Central Indian Tectonic zone: Implications on the time of amalgamation of the North and South Indian Blocks. *J. Asian Earth Sci.* **2025**, *2025*, 106799. https://doi.org/10.1016/j.jseaes.2025.106799
8. Bhowmik, S.K. The current status of orogenesis in the Central Indian Tectonic Zone: A view from its Southern Margin. *Geol. J.* **2019**, *54*, 2597–2620. https://doi.org/10.1002/gj.3456
9. Chattopadhyay, A.; Bhowmik, S.K.; Roy, A. Tectonothermal evolution of the Central Indian Tectonic Zone and its implications for Proterozoic supercontinent assembly: The current status. *Episodes* **2020**, *43*, 132–144. https://doi.org/10.18814/epiiugs/2020/020008

10. Naganjaneyulu, K.; Santosh, M. The Central India Tectonic Zone: A geophysical perspective on continental amalgamation along a Meso-Proterozoic suture. *Gond. Res.* **2010**, *18*, 547–564.
11. Deshmukh, T.; Naraga, P.; Bhattacharya, A. Proterozoic HT–LP metamorphism in the Mahakoshal Belt, Central Indian Tectonic Zone (India): Structure, metamorphism, U–Th–Pb monazite geochronology and tectonic implications. *J. Geol.* **2021**, *129*, 455–480. https://doi.org/10.1086/715772
12. Giri, R.; Chalapathi Rao, N.V.; Rahaman, W.; et al. Paleoproterozoic calc-alkaline lamprophyres from the Sidhi Gneissic complex, India: Implications for plate tectonic evolution of the Central Indian Tectonic Zone. *Precambrian Res.* **2021**, *362*, 106316. https://doi.org/10.1016/j.precamres.2021.106316
13. Mahakud, S.P.; Raut, P.K.; Hansda, C.; et al. *Sulfide Mineralization in the Central Part of the Betul Belt around Ghisi-Mouriya-Koparpani Area, Betul District, Madhya Pradesh*; Geological Survey of India: Kolkata, India, 2001; Volume 64, pp. 377–385.
14. Tripathi, S.; Deb, M. Decoding imprints of hydrothermal alteration around Imalia polymetallic sulphide deposit, Central Indian Tectonic Zone, and its implications on ore genesis. *Geol. Mag.* **2025**, *162*, 12–30. https://doi.org/10.1017/S0016756825000056
15. Misra, P.S.; Singh, V.; Tripathi, U.; et al. Gold Mineralization in Eastern Mahakoshal Belt of Central India: A Reappraisal Based on Mineral System. *J. Geol. Soc. India* **2023**, *97*, 985–992. https://doi.org/10.1007/s12594-021-1813-0
16. Baswani, S.R.; Hazarika, P.; Meshram, T.; et al. Genesis of Greenockite (CdS) and associated sulfide-gold mineralization from Mahakoshal Belt, Central Indian Tectonic Zone. *Geol. J.* **2023**, *58*, 1623–1643. https://doi.org/10.1002/gj.4681
17. Golani, P.R.; Dora, M.L.; Bandyopadhyay, B.K. Base metal mineralization associated with hydrothermal alteration in felsic volcanic rocks in Proterozoic Betul Belt at Bhuyari, Chhindwara district, Madhya Pradesh. *J. Geol. Soc. India* **2006**, *68*, 797–808.
18. Roy, S. Possible VMS-type base metal mineralization at Pastalaimal and associated alteration features: Implications for identification of future targets in Betul belt, Madhya Pradesh, India. *J. Geol. Soc. India* **2011**, *77*, 459–464. https://doi.org/10.1007/s12594-011-0104-5
19. Praveen, M.N.; Nambiar, C.G.; Huston, D.L. Geochemistry and petrogenesis of Paleoproterozoic rhyolite-hosted zinc-rich metamorphosed volcanogenic massive sulfide deposits in the eastern Betul Belt, central India. *Ore Geol. Rev.* **2021**, *131*, 103918. https://doi.org/10.1016/j.oregeorev.2020.103918
20. Sharma, R.K.; Lenka, B.; Ahmed, S. Genesis of Graphite in Betul Belt, Madhya Pradesh, India: Inferences Based on Petrographic and Other Studies. *Open J. Geol.* **2022**, *12*, 983–1012. https://doi.org/10.4236/ojg.2022.1211047
21. Patel, V.V.; Sahu, P.K.; Talwar, A.K. Graphite within Carbonaceous Phyllite, Mahakoshal Group, Central Indian Tectonic Zone. *Curr. Sci.* **2021**, *121*, 192–195. https://doi.org/10.18520/cs/v121/i2/192-195
22. Patro, P.K.; Vijaya Kumar, P.V.; Abhirami, S.G.; et al. Integrated subsurface investigation for magmatic sulfide mineralization in Betul Fold Belt, central India. *J. Appl. Geophys.* **2023**, *211*, 104974. https://doi.org/10.1016/j.jappgeo.2023.104974
23. Meshram, R. R.; Mohamed, S. Geology and Genesis of pegmatites of Parseoni areas in Sausar Mobile Belt, Nagpur district, Central India. *Indian J. Geosci.* **2019**, *73*, 119–130.
24. Naqvi, S.M.; Rogers, J.J.W. *Precambrian Geology of India*; Oxford University Press: Oxford, UK, 1987; 233p.
25. Roy, A.; Prasad, M.H. Tectonothermal events in Central Indian Tectonic Zone (CITZ) and its implications in Rodinian crustal assembly. *J. Asian Earth Sci.* **2003**, *22*, 115–129. https://doi.org/10.1016/S1367-9120(02)00180-3
26. GSI. *Geology and Mineral Resources of Madhya Pradesh* (3rd ed.); GSI Misc Pub, No 30, Part-XI; GSI: Kolkata, India, 2014.
27. GSI. *Geology and Mineral Resources of Maharashtra* (3rd ed.); GSI Misc Pub, No 30, Part-II; GSI: Kolkata, India, 2016.
28. Wani, H.; Mondal, M. Geochemical evidence for the Paleoproterozoic arc–back arc basin association and its importance in understanding the evolution of the Central Indian Tectonic Zone. *Tectonophysics* **2016**, *690*, 57–67. https://doi.org/10.1016/j.tecto.2016.10.001
29. Bhandari, A.; Pant, N.C.; Bhowmik, S.K.; et al. 1.6 Ga ultrahigh-temperature granulite metamorphism in the Central Indian Tectonic Zone: Insights from metamorphic reaction history, geothermobarometry and monazite chemical ages. *Geol. J.* **2011**, *46*, 198–216. https://doi.org/10.1002/gj.1244
30. Yedekar, D.B.; Jain, S.C.; Nair, K.K.K.; et al. 1990. *The Central Indian Collision Suture*; Special Publication 28, 1–Acharyya; Geological Survey of India: Kolkata, India, 2003.
31. Acharyya, S.K. The nature of Mesoproterozoic Central Indian Tectonic Zone with exhumed and reworked older granulites. *Gondwana Res.* **2003**, *6*, 197–214. https://doi.org/10.1016/S1342-937X(05)70970-9
32. Bhowmik, S.K.; Chakraborty, S. Sequential kinetic modelling: A new tool decodes pulsed tectonic patterns in early hot orogens of Earth. *Earth Planet. Sci. Lett.* **2017**, *460*, 171–179. https://doi.org/10.1016/j.epsl.2016.12.018
33. Nair, K.; Jain, S.; Yedekar, D. Stratigraphy, structure and geochemistry of the Mahakoshal greenstone belt. *Mem. Geol. Soc. India* **1995**, *37*, 403–432.
34. Roy, A.; Devarajan, M.K. Appraisal of the stratigraphy and tectonics of the Proterozoic Mahakoshal supracrustals belt, central India. *Geol. Surv. India Spl. Pub* **2000**, *57*, 79–97

35. Khan, M.A. *Gold mineralization in Son Valley Gold Belt, Parts of Sidhi and Sonbhadra Districts, Madhya Pradesh and Uttar Pradesh*; Bulletin Series-A, No. 61; Geological Survey of India: Kolkata, India, 2013
36. Giri, R.K.; Pandit, D.; Chalapathi Rao, N.V. Cobaltoan pyrite in a lamprophyre from the Sidhi Gneissic complex, Mahakoshal belt, Central India. *J Geol Soc India* **2018**, *91*, 5–8. https://doi.org/10.1007/s12594-018-0813-1
37. Srivastava, R.K.; Chalapathi Rao, N.V. Petrology, geochemistry and tectonic significance of Palaeoproterozoic alkaline lamprophyres from the Jungel Valley, Mahakoshal Supracrustal Belt, Central India. *Mineral. Petrol.* **2007**, *89*, 189–215.
38. Parvez, K.; Mondal, M.E.A.; Ahmad Iftikhar Rahaman, W.; et al. Mineralogical, Geochemical and Nd Isotopic Study of the Meta-Clastic Rocks of the Paleoproterozoic Mahakoshal Basin, Central Indian Tectonic Zone: Implications for Provenance Characterization, Paleoweathering Conditions and Tectonic Setting. *Geochem. Int.* **2024**, *62*, 1378–1404. https://doi.org/10.1134/S0016702924700472
39. Khanna, T.; Rao, D.V.; Sai, V.V.; et al. ca. 2.1 Ga Mahakoshal Supracrustal Belt: An allochthonous terrain in Central India Tectonic Zone. *Lithos* **2020**, *374–375*, 105705. https://doi.org/10.1016/j.lithos.2020.105705
40. Chakrabarty, A.; Shreya, K.; Subham, M.; et al. Neoproterozoic reworking of a Mesoproterozoic magmatic arc from the north-eastern part of the Central Indian Tectonic Zone: Implication for the growth and disintegration of the Indian shield in the Proterozoic supercontinental cycles. *Precambrian Res.* **2022**, *378*, 106758. https://doi.org/10.1016/j.precamres.2022.106758
41. Radhakrishna, B.P.; Naqvi, S.M. Precambrian continental crust of India and its evolution. *J. Geol.* **1986**, *94*, 145–166. https://doi.org/10.1086/629018
42. Yadav, B.; Ahmad, T.; Kaulina, T.; et al. Origin of post-collisional A-type granites in the Mahakoshal Supracrustal Belt, Central Indian Tectonic Zone, India:Zircon U–Pb ages and geochemical evidences. *J. Asian Earth Sci.* **2020**, *191*, 104274. https://doi.org/10.1016/j.jseaes.2020.104274
43. Bora, S.; Kumar, S. Geochemistry of biotites and host granitoid plutons from the Proterozoic Mahakoshal Belt, central India tectonic zone: Implication for nature and tectonic setting of magmatism. *Int. Geol. Rev.* **2015**, *57*, 1686–1706. https://doi.org/10.1080/00206814.2015.1032372
44. Chaturvedi, R.K. A review of the Geology, Tectonic features and tectono-lithostratigraphy of Betul Belt. *Geol. Surv. India Spec. Publ.* **2001**, *64*, 299–315.
45. Chore, S.A.; Chakraborty, S.; Vishwakarma, L.L.; et al. Petrology of base metal bearing volcano sedimentary litho assemblages of the Betul Belt of Central India and its possible significance in the evolutionary history of the Central Indian Tectonic Zone. *Surv. Rec.* **2002**, *135*, 16–17.
46. Roy, A.; Chakraborti, K.Precambrian Mafic-Ultramafic Magmatism in Central Indian Suture Zone. *J. Geol. Soc. India* **2008**, *72*, 123–140.
47. Dora, M.L.; Helmy, H.M.; Meshram, R.; et al. Proterozoic arc magmatism from the Padhar mafic-ultramafics in Betul Belt, Central India Tectonic Zone: Insight from petrography, bulk rock and in-situ trace element geochemistry. Geo*syst. Geoenviron.* **2025**, 100383. https://doi.org/10.1016/j.geogeo.2025.100383
48. Ghosh, B.; Praveen, M.N. Indicator minerals as guides to base metal sulfide mineralization in Betul Belt, central India. *J. Earth Syst. Sci.* **2008**, *117*, 521–536. https://doi.org/10.1007/s12040-008-0050-x
49. Raza, M.A.; Shareef, M.; Naidu, B.V.S.S.A.; et al. Multiple sulfur sources for the volcanic hosted massive sulfides in Betul Belt, Central India: Evidence from the sulfide ore chemistry and sulfur isotope geochemistry. *Geochemistry* **2020**, *80*, 125632. https://doi.org/10.1016/j.chemer.2020.125632
50. Sharma, A.; Das, K.; Chakraborty, P.P.; et al. U–Pb zircon geochronology of a pyroclastic rock from the Parsoi Formation, Mahakoshal Group: Implications towards age and tectonics of the Basin in Central Indian Tectonic Zone. *Geol. J.* **2022**, *57*, 4122–4138. https://doi.org/10.1002/gj.4533
51. Baswani, S.R.; Mishra, B.P.; Mahapatro, S.N.; et al. Petrochemical evaluation of gahnite from volcanogenic massive sulfide deposits in Betul belt, Central India: Insight from petrography and in-situ trace element geochemistry. *Geol. J.* **2022**, *57*, 4508–4528. https://doi.org/10.1002/gj.4555
52. Narayanaswami, S.; Chakravarty, S.C.; Vemban, N.A.; et al. *The Geology and Manganese Ore Deposits of the Manganese Belt in Madhya Pradesh and Adjoining Parts of Maharashtra*; Bulletin Geological Survey of India, Series A; GSI: Kolkata, India, 1963.
53. Dasgupta, S.; Roy, S.; Fukuoka, M. Depositional models for manganese oxide and carbonate deposits of the Precambrian Sausar Group, India. *Econ. Geol.* **1992**, *87*, 1412–1418. https://doi.org/10.2113/gsecongeo.87.5.1412
54. Chattopadhyay, A.; Khan, S.; Huin, A.K.; et al. Reinterpretation of stratigraphy and structure of Sausar Group in Ramtek–Mansar–Kandri area, Maharashtra, central India. *J. Geol. Soc. India* **2003**, *6*, 75–89
55. Mohanty, S.P. Spatio-temporal evolution of the Satpura Mountain Belt of India: A comparison with the Capricorn Orogen of Western Australia and implication for evolution of the supercontinent Columbia. *Geosci. Front.* **2012**, *3*, 241–267. https://doi.org/10.1016/j.gsf.2011.12.004
56. Jawed, T.; Siddiquie, F.N. Mineragraphic Study of Manganese Ore Deposits of Kandri, Mansar, Beldongri and Satak Mines, Nagpur District (Maharashtra), Central India. *Int. J. Geosci.* **2014**, *5*, 710–727. https://doi.org/10.4236/ijg.2014.57064

57. Devarajan, M.K.; Prasad, M.H.; Prasad, K.A.V.; et al. Gold mineralization in the Mahakoshal Greenstone Belt, Central India: A preliminary study. *J. Geol. Soc. India* **1998**, *52*, 147–152.
58. Tripathi, U.; Deb, M. Mineralogy of the Imalia Au-Sn-bearing polymetallic sulfide deposit, Mahakoshal belt, Central India. *J. Asian Earth Sci. X* **2022**, *8*, 100117. https://doi.org/10.1016/j.jaesx.2022.100117
59. Yousuf, I.; Ahmad, T.; Subba Rao, D.V.; et al. Geochemistry, geochronology and petrogenesis of the Proterozoic Betul–Chhindwara bimodal volcanics: Constraints on the evolution of the Central Indian Tectonic Zone. *Geol. J.* **2025**, *60*, 1701–1720. https://doi.org/10.1002/gj.5154
60. Raut, P.K.; Mahakud, S.P. Geology, geochemistry and tectonic setting of the volcanosedimentary sequence of Betul belt, Madhya Pradesh and genesis of zinc and copper sulfide mineralization. *Geol. Surv. India Spl. Pub* **2004**, *72*, 133–146.
61. Praveen, M.N.; Ghosh, B.; Shrivastava Dora, M.L.; et al. Sulfide mineralization in Betul Bel: Classification and general characteristics. *Geol. Soc. India* **2007**, *69*, 85–91.
62. Mishra, B.P.; Pati, P.; Dora, M.L.; et al. Trace-element systematics and isotopic characteristics of sphalerite–pyrite from volcanogenic massive sulfide deposits of Betul belt, Central Indian Tectonic Zone: Insight of ore genesis to exploration. *Ore Geol. Rev.* **2021**, *134*, 104149. https://doi.org/10.1016/j.oregeorev.2021.104149
63. Rao, D.S.; Satyanarayanan, M.; Sarma, D.S.; et al. Geochemistry of the unusual mafic intrusions in Betul Fold Belt, Central India: Implications for Ni–Cu–Au–PGE metallogeny. *Curr. Sci.* **2015**, *108*, 713–722.
64. Dhillon, S.; Balaram, V.; Kishore, N.; et al. Petrography and geochemistry of padhar mafic-ultramafic suite rocks, Betul Belt, Central Indian Tectonic Zone, India: Plausible arc type magmatism. *IOSR J. Appl. Geol. Geophy.* **2017**, *5*, 53–61.
65. Kanungo, D.R.; Malpe, D.B.; Leake, B.E. Manganocummingtonite from the Mesoproterozoic, Sausar Fold Belt, Central India. *J. Geol. Soc. India* **2014**, *83*, 93–99. https://doi.org/10.1007/s12594-014-0011-8
66. Chattopadhyay, A.; Chatterjee, A.; Das, K.; et al. Neoproterozoic transpression and granite magmatism in the Gavilgarh–Tan Shear Zone, central India: Tectonic significance of U-Pb zircon and U-Th-total Pb monazite ages. *J. Asian Earth Sci.* **2017**, *147*, 485–501. https://doi.org/10.1016/j.jseaes.2017.08.018
67. Meshram, R.R.; Rao, N.R.; Chore, S.; et al. The Alaskan-type mafic-ultramafic complex at Padhar, Betul Belt, Central India. *Curr. Sci.* **2018**, *114–113*, 671–678.
68. Roy, A.; Kagami, H.; Yoshida, M.; et al. Rb–Sr and Sm–Nd dating of different metamorphic events from the Sausar mobile belt, central India: Implications for Proterozoic crustal evolution. *J. Asian Earth Sci.* **2006**, *26*, 61–76. https://doi.org/10.1016/j.jseaes.2004.09.010
69. Singh, P.K.; Verma, S.K.; Singh, V.K.; et al. Geochronology and petrogenesis of the TTG gneisses and granitoids from the Central Bundelkhand granite–greenstone terrane, Bundelkhand Craton, India: Implications for Archean crustal evolution and cratonization. *Precambrian Res.* **2021**, *359*, 106210. https://doi.org/10.1016/j.precamres.2021.106210
70. Mandal, B.; Sen, M.K.; Vijaya Rao, V. New seismic images of the Central Indian Suture Zone and its tectonic implications. *Tectonics* **2013**, *32*, 908–921.
71. Santosh, M.; Groves, D.I. Global metallogeny in relation to secular evolution of the Earth and supercontinent cycles. *Gondwana Res.* **2022**, *106*, 1–24. https://doi.org/10.1016/j.gr.2022.06.001
72. Groves, D.I.; Vielreicher, R.M.; Goldfarb, R.J.; et al. Controls on the heterogeneous distribution of mineral deposits through time. In *Mineral Deposits and Earth Evolution*; McDonald, I, Boyce, A.J., Butler, I.B., et al., Eds.; Geological Society of London: London, UK, 2005; Volume 248, pp. 71–102.
73. Goldfarb, R.J.; Baker, T.; Dubé, B; et al. Distribution, character, and genesis of gold deposits in metamorphic terranes. In *One Hundredth Anniversary Volume*; Society of Economic Geologists: Littleton, CO, USA, 2005; pp. 407–450.
74. Goldfarb, R.J.; André-Mayer, A.-S.; Jowitt, S.; et al. West Africa: The world's premier Paleoproterozoic gold province. *Econ. Geol.* **2017**, *112*, 121–143. https://doi.org/10.2113/econgeo.112.1.121
75. Dhopeshwar, S.V.; Khare, M.S.; Shrivastava, J. A behavioral analysis of iron and silica in iron ore deposits of parts of Mahakoshal & Bijawar region, Madhya Pradesh. *Int. J. Adv. Res.* **2017**, *5*, 614–629. https://doi.org/10.21474/IJAR01/4457
76. Franklin, J.M.; Gibson, H.L.; Jonasson, I.R.; et al. Volcanogenic massive sulfide deposits. *In Economic Geology 100th Anniversary Volume*; Hedenquist, J.W., Thompson, J.F.H., Goldfarb, R.J., et al., Eds.; Society of Economic Geologists: Littleton, CO, USA, 2005; pp. 523–560. https://doi.org/10.5382/AV100.17
77. Schaefer, M.O.; Gutzmer, J.; Beukes, N.J. Late Paleoproterozoic Mn-rich oncoids: Earliest evidence for microbially mediated Mn precipitation. *Geology* **2001**, *29*, 835–838.
78. Srivastava, R.K.. *Petrogenesis and tectonic significance of the mafic volcanic rocks of the Mahakoshal Belt, Central India. J. Geol. Soc. India* **2006**, *68*, 369–386.
79. Rogers, J.J.W.; Santosh, M. Configuration of Columbia, a Mesoproterozoic supercontinent. *Gondwana Res.* **2002**, *5*, 5–22. https://doi.org/10.1016/S1342-937X(05)70883-2
80. Kusky, T.M.; Santosh, M. *The Columbia connection in North China*; Geological Society of London: London, UK, 2009; Volume 323, pp. 49–71. https://doi.org/10.1144/SP323.3
81. Pirajno, F. Metallogeny in the Capricorn Orogen, Western Australia, the result of multiple ore-forming

processes. *Precambrian Res.* **2004**, *128*, 411–439. https://doi.org/10.1016/j.precamres.2003.09.010

82. Kasturi Rangan, K.; Santosh, M. Tectonics and metallogeny of Proterozoic orogens: A global perspective. *Gondwana Res.* **2010**, *18*, 167–188.
83. Granseth, A.; Slagstad, T.; Roberts, N.M.W.; et al. Multi-isotope tracing of the 1.3–0.9 Ga evolution of Fennoscandia; crustal growth during the Sveconorwegian orogeny. *Gondwana Res.* **2021**, *91*, 31–39. https://doi.org/10.1016/j.gr.2020.10.019
84. Bose, S.; Das, K.; Torimoto, J.; et al. Evolution of the Chilka Lake granulite complex, northern Eastern Ghats Belt, India: First evidence of ~780 Ma decompression of the deep crust and its implication on the India–Antarctica correlation. *Lithos* **2016**, *263*, 161–189. https://doi.org/10.1016/j.lithos.2016.01.017
85. Sangster, D.F.; Franklin, J.M.; Lydon, J.W. Volcanogenic massive sulfide deposits. In *Geology of Canadian Mineral Deposit Types*; Paper 88-21; Geological Survey of Canada: Ottawa, ON, Canada, 1992; pp. 125–140.
86. Goodenough, K.M.; Wall, F.; Merriman, D. The Rare Earth Elements: Demand, Global Resources, and Challenges for Resourcing Future Generations. *Nat. Resour. Res.* **2018**, *27*, 201–216. https://doi.org/10.1007/s11053-017-9336-5